PROXIMAL METHODS FOR IMAGE RESTORATION USING A CLASS OF NON-TIGHT FRAME REPRESENTATIONS

Nelly Pustelnik, Jean-Christophe Pesquet and Caroline Chaux

Université Paris-Est
Laboratoire d'Informatique Gaspard Monge, UMR CNRS 8049
77454 Marne-la-Vallée Cedex, France
phone: + (33) 1 60 95 72 92, fax : +(33) 1 60 95 75 57
e-mail: {nelly.pustelnik,jean-christophe.pesquet,caroline.chaux}@univ-paris-est.fr

ABSTRACT

The objective of this paper is to develop a convex optimization approach for solving image deconvolution problems involving frame representations. Until now, most of the proposed frame-based variational methods assumed either Lipschitz differentiability properties or tight representations. These assumptions are relaxed here, thus offering the possibility of considering a broader class of image restoration problems. The proposed algorithms allow us to solve both frame analysis and frame synthesis problems for various noise distributions. The proposed approach is proved to be effective for restoring data corrupted by Poisson noise by using (non-tight) discrete dual-tree wavelet representations.

1. INTRODUCTION

Many works in image processing are concerned with challenging inverse problems such as denoising or deconvolution. For such problems, the original image $\overline{y} \in \mathbb{R}^N$ is degraded by a matrix $T \in \mathbb{R}^{N\times N}$ modeling a convolutive degradation and by a non-necessarily additive noise. The resulting degradation model is the following:

$$z = \mathscr{D}_\alpha(T\overline{y}) \tag{1}$$

where $\mathscr{D}_\alpha$ denotes the noise effect and $\alpha > 0$ is some related parameter (for example, α may represent the variance for Gaussian noise or the scaling parameter for Poisson noise). In this context, our objective is to recover an image $y \in \mathbb{R}^N$, the closest possible to $\overline{y}$, from the observation vector $z \in \mathbb{R}^N$ and available prior information. In early works, this problem was solved for Gaussian noise using Wiener filtering, or equivalently quadratic regularization techniques. Later, multiresolution analyses were used for denoising by applying a thresholding to the generated coefficients [1]. Then, in order to improve the denoising performance, redundant frame representations were substituted for wavelet bases [2]. In [3, 4, 5, 6], authors considered convex optimization techniques to jointly address the effects of a noise and of a linear degradation within a convex variational framework. When the noise is Gaussian, the forward-backward (FB) algorithm [3] (also known as thresholded Landweber when the regularization term is an ℓ_1-norm [4, 5, 6]) can be employed in the context of wavelet basis decompositions and its use can be extended to arbitrary frame representations [7]. However, in the context of a non-additive noise such as a Poisson noise or a Laplace noise, FB algorithm is no longer applicable due to the non-Lipschitz differentiability of the data fidelity term. Other convex optimization algorithms must be employed such as the Douglas-Rachford (DR) algorithm [8], the Parallel Proximal Algorithm (PPXA) [9] or the Alternating Direction Method of Multipliers (ADMM) [10, 11]. Nevertheless, for tractability issues, the authors have restricted the scope of their works to tight frame representations [9, 10, 11]. The goal of this paper is to propose a way to relax the tight frame requirement by considering a particular class of frame representations.

In the following, we consider two convex minimization problems which are useful to solve frame-based restoration problems formulated under a Synthesis Form (SF) or an Analysis Form (AF). The SF can be expressed as:

$$\underset{y=F^\top x,\, x\in\mathbb{R}^K}{\text{minimize}} \sum_{i=1}^{n} f_i(L_i y) + \sum_{j=1}^{m} g_j(x) \tag{2}$$

and the AF is:

$$\underset{y\in\mathbb{R}^N}{\text{minimize}} \sum_{i=1}^{n} f_i(L_i y) + \sum_{j=1}^{m} g_j(Fy). \tag{3}$$

$F \in \mathbb{R}^{K\times N}$ (resp. $F^\top \in \mathbb{R}^{N\times K}$) denotes the frame analysis (resp. synthesis) operator. For every $i \in \{1,\dots,n\}$, $f_i\colon \mathbb{R}^N \mapsto]-\infty,+\infty]$ is a convex, lower semicontinuous and proper function and $L_i \in \mathbb{R}^{N\times N}$ is a convolutive operator. For every $j \in \{1,\dots,m\}$, $g_j\colon \mathbb{R}^K \mapsto]-\infty,+\infty]$ is a convex, lower semicontinuous and proper function. In numerous works, SF is prefered since AF appears more difficult to solve numerically [12, 13, 14].

This paper is organized as follows: Section 2 presents the structure of the frames considered in this work. Section 3 recalls convex optimization tools such as proximity operators and describes the proposed algorithms to minimize (2) and (3). Finally, restoration results are given in Section 4 in the presence of Poisson noise, by using Dual-Tree Transforms (DTT).

Notation: Throughout this paper, $\Gamma_0(\mathbb{R}^I)$ designates the class of lower semicontinuous convex functions $\varphi\colon \mathbb{R}^I \to]-\infty,+\infty]$ which are proper in the sense that their domain $\operatorname{dom}\varphi = \{u \in \mathbb{R}^I \mid \varphi(u) < +\infty\}$ is nonempty. If $\varphi \in \Gamma_0(\mathbb{R}^I)$ has a unique minimizer, it is denoted by $\operatorname{argmin}_{u\in\mathbb{R}^I} \varphi(u)$. The relative interior of a set S is denoted by $\operatorname{ri} S$.

2. FRAME REPRESENTATIONS

Physical properties of the target image $\overline{y}$, such as sparsity or spatial regularity, are suitably expressed in terms of the frame coefficients $\overline{x} = (\overline{x}^{(k)})_{1\leq k\leq K} \in \mathbb{R}^K$ where $\overline{y} = \sum_{k=1}^K \overline{x}^{(k)} e_k$ and $(e_k)_{1\leq k\leq K}$ denotes a family of vectors in the Euclidean space $\mathbb{R}^N$ ($N \leq K$). Such a family of vectors constitutes a frame if there exists a constant μ in $]0,+\infty[$ such that

$$(\forall y \in \mathbb{R}^N) \qquad \mu \|y\|^2 \leq \sum_{k=1}^K |\langle y \mid e_k\rangle|^2. \tag{4}$$

The associated frame operator is the injective linear operator defined as

$$(\forall y \in \mathbb{R}^N) \qquad Fy = (\langle y \mid e_k\rangle)_{1\leq k\leq K}, \tag{5}$$

the adjoint of which is the surjective linear operator given by

$$\left(\forall (x^{(k)})_{1\leq k\leq K} \in \mathbb{R}^K\right) \quad F^\top (x^{(k)})_{1\leq k\leq K} = \sum_{k=1}^K x^{(k)} e_k. \tag{6}$$

2.1 Tight frames

A tight frame is such that

$$F^\top F = \mu \mathrm{I}, \qquad \mu \in]0,+\infty[, \tag{7}$$

where I denotes the identity matrix. A simple example of a tight frame is the union of μ orthonormal bases. Other examples of tight frames can be found in [15, 16, 17]. When $F^{-1} = F^\top$, an orthonormal basis is obtained. Further constructions as well as a detailed account of frame theory in Hilbert spaces can be found in [18].

2.2 A particular class of non tight frames

A subclass of frame representations is defined as

$$F = U \begin{bmatrix} V_1 \\ V_2 \\ \vdots \\ V_Q \end{bmatrix} \tag{8}$$

where, $U \in \mathbb{R}^{K\times QN}$ is a tight frame analysis matrix with constant $\mu_U \in]0,+\infty[$, and for every $q \in \{1,\ldots,Q\}$, $V_q \in \mathbb{R}^{N\times N}$ is a prefiltering operator . For Condition (4) to be fullfilled, prefilters $(V_q)_{1\leq q\leq Q}$ must satisfy the following lower boundedness relation:

$$(\forall \omega \in [-\pi,\pi]^2) \qquad \mu_U \sum_{q=1}^Q |\hat{v}_q(\omega)|^2 \geq \mu, \tag{9}$$

where, for every $q \in \{1,\ldots,Q\}$, $\hat{v}_q(\omega)$ denotes the frequency response of the filter associated with the convolutive operator V_q. Indeed, it is straightforward to show that

$$F^\top F = \mu_U \sum_{q=1}^Q V_q^\top V_q. \tag{10}$$

The simplest example of such a frame is a Q-channel undecimated filter bank satisfying (9), which has a redundancy of a factor Q. In order to obtain low redundancy representations, frames such as the 2D real (resp. complex) M-band DTT have been proposed [19, 20]. The DTT consists of performing two (resp. four) M-band orthonormal wavelet decompositions in parallel (orthogonal matrices U_q), each one being preceded by a prefiltering stage (V_q matrices) related to discretization. Finally, an orthogonal combination (orthogonal matrix R) of the subbands is applied to ensure directionality. Such a frame satisfies (8) and (9), where

$$U = R \begin{bmatrix} U_1 & 0 & \ldots & 0 \\ 0 & U_2 & \ldots & 0 \\ \vdots & & \ddots & \vdots \\ 0 & \ldots & \ldots & U_Q \end{bmatrix}. \tag{11}$$

Note that the *discrete* DTT is not a tight frame in general.

Tight frame representations have been widely used in convex optimization methods for data recovery. In the next section, we recall some convex optimization tools and show the relevance of the class of frames defined by (8) in conjunction with recent optimization approaches.

3. PROXIMAL TOOLS AND ALGORITHMS

In imaging, there has been recently a growing interest in advanced convex optimization tools. A commonly used tool is the Projection Onto Convex Sets (POCS) which is an alternating projection algorithm. The notion of projection was extended by Moreau [21] by introducing the proximity operator of a function $\varphi \in \Gamma_0(\mathbb{R}^I)$:

$$\mathrm{prox}_\varphi \colon \mathbb{R}^I \to \mathbb{R}^I \colon v \mapsto \arg\min_{u\in\mathbb{R}^I} \frac{1}{2}\|u-v\|^2 + \varphi(u). \tag{12}$$

It can be observed that when φ is the indicator function ι_C of a nonempty closed convex subset C of $\mathbb{R}^I$, i.e.

$$(\forall u \in \mathbb{R}^I) \quad \varphi(u) = \begin{cases} 0, & \text{if } u \in C; \\ +\infty, & \text{otherwise,} \end{cases} \tag{13}$$

prox_{ι_C} reduces to the projector P_C onto C. Other examples of proximity operators corresponding to the potential functions of standard log-concave univariate probability densities have been listed in [3, 7, 9]. The proximity operators used in the experimental part of this paper, are recalled below.

Example 3.1 *Let $\chi > 0$, and set*

$$\varphi \colon \mathbb{R} \to]-\infty,+\infty] \colon \xi \mapsto \chi|\xi|. \tag{14}$$

Then, for every $\xi \in \mathbb{R}$,

$$\mathrm{prox}_\varphi \xi = \mathrm{sign}(\xi)\max\{|\xi| - \chi, 0\}. \tag{15}$$

Example 3.2 [7]
Let $\alpha > 0$, and set

$$\varphi \colon \mathbb{R} \to]-\infty,+\infty]$$
$$\xi \mapsto \begin{cases} -\chi\ln(\xi) + \alpha\xi, & \text{if } \chi > 0 \text{ and } \xi > 0; \\ \alpha\xi, & \text{if } \chi = 0 \text{ and } \xi \geq 0; \\ +\infty, & \text{otherwise.} \end{cases} \tag{16}$$

Then, for every $\xi \in \mathbb{R}$,

$$\operatorname{prox}_{\varphi}\xi = \frac{\xi-\alpha+\sqrt{|\xi-\alpha|^2+4\chi}}{2}. \tag{17}$$

Numerous iterative algorithms are based on proximity operators such as FB or DR algorithms allowing us to minimize a sum of two functions with secured convergence properties. The former one can be regarded as more restrictive than the latter one in the sense that it requires the Lipschitz differentiability of one function. To solve the considered minimization problems formulated in (2) and (3), two solutions can be considered. On the one hand, DR formulation in a product space leads to the PPXA algorithm presented in [9] for minimizing a sum of more than two convex functions. However, one of the difficulties of the considered minimization problems formulated in (2) and (3) is that they involve linear operators. A solution consists of using the following result:

Proposition 3.3 [8]
Let $\varphi \in \Gamma_0(\mathbb{R}^J)$ *and let* $L \in \mathbb{R}^{J\times I}$. *Suppose that* $LL^\top = \chi \mathrm{I}$, *for some* $\chi \in]0,+\infty[$. *Then,* $\varphi \circ L \in \Gamma_0(\mathbb{R}^I)$ *and*

$$\operatorname{prox}_{\varphi\circ L} = \mathrm{I} + \chi^{-1}L^\top(\operatorname{prox}_{\chi\varphi} - \mathrm{I})L. \tag{18}$$

On the other hand, augmented Lagrangian algorithms such as ADMM (sometimes also named alternating split Bregman algorithm) can be used [10, 11]. Both solutions are considered in the literature for dealing with tight frame representations.

In [22], it is shown that PPXA and ADMM can be put in a unifying framework based on proximity operators. The application of the resulting algorithm (called PPXA+) to Problem (2) (resp. Problem (3)) is given in Algorithm 1 (resp. Algorithm 2). (In these algorithms, the sequences $(a_{i,\ell})_{1\le i\le n}$ and $(b_{j,\ell})_{1\le j\le m}$ correspond to possible numerical errors in the computation of the proximity operators at iteration ℓ.)

Algorithm 1

Initialization
- $(\eta_i)_{1\le i\le n} \in]0,+\infty[^n$, $(\kappa_j)_{1\le j\le m} \in]0,+\infty[^m$
- $(v_{i,0})_{1\le i\le n} \in (\mathbb{R}^N)^n$, $(w_{j,0})_{1\le j\le m} \in (\mathbb{R}^K)^m$
- $x_0 = \operatorname{arg\,min}_{u\in\mathbb{R}^K} \sum_{i=1}^n \eta_i \|L_i F^\top u - v_{i,0}\|^2 + \sum_{j=1}^m \kappa_j \|u - w_{j,0}\|^2$

For $\ell = 0,1,\ldots$
- For $i = 1,\ldots,n$
  - $p_{i,\ell} = \operatorname{prox}_{f_i/\eta_i} v_{i,\ell} + a_{i,\ell}$
- For $j = 1,\ldots,m$
  - $r_{j,\ell} = \operatorname{prox}_{g_j/\kappa_j} w_{j,\ell} + b_{j,\ell}$
- $\lambda_\ell \in]0,2[$
- $c_\ell = \operatorname{arg\,min}_{u\in\mathbb{R}^K} \sum_{i=1}^n \eta_i \|L_i F^\top u - p_{i,\ell}\|^2 + \sum_{j=1}^m \kappa_j \|u - r_{j,\ell}\|^2$
- For $i = 1,\ldots,n$
  - $v_{i,\ell+1} = v_{i,\ell} + \lambda_\ell\big(L_i F^\top (2c_\ell - x_\ell) - p_{i,\ell}\big)$
- For $j = 1,\ldots,m$
  - $w_{j,\ell+1} = w_{j,\ell} + \lambda_\ell\big(2c_\ell - x_\ell - r_{j,\ell}\big)$
- $x_{\ell+1} = x_\ell + \lambda_\ell(c_\ell - x_\ell)$

The convergence of the sequence $(x_\ell)_{\ell\in\mathbb{N}}$ (resp. $(y_\ell)_{\ell\in\mathbb{N}}$) generated by Algorithm 1 (resp. Algorithm 2) is established under the following assumptions:

Algorithm 2

Initialization
- $(\eta_i)_{1\le i\le n} \in]0,+\infty[^n$, $(\kappa_j)_{1\le j\le m} \in]0,+\infty[^m$
- $(v_{i,0})_{1\le i\le n} \in (\mathbb{R}^N)^n$, $(w_{j,0})_{1\le j\le m} \in (\mathbb{R}^K)^m$
- $y_0 = \operatorname{arg\,min}_{u\in\mathbb{R}^N} \sum_{i=1}^n \eta_i \|L_i u - v_{i,0}\|^2 + \sum_{j=1}^m \kappa_j \|F u - w_{j,0}\|^2$

For $\ell = 0,1,\ldots$
- For $i = 1,\ldots,n$
  - $p_{i,\ell} = \operatorname{prox}_{f_i/\eta_i} v_{i,\ell} + a_{i,\ell}$
- For $j = 1,\ldots,m$
  - $r_{j,\ell} = \operatorname{prox}_{g_j/\kappa_j} w_{j,\ell} + b_{j,\ell}$
- $\lambda_\ell \in]0,2[$
- $c_\ell = \operatorname{arg\,min}_{u\in\mathbb{R}^N} \sum_{i=1}^n \eta_i \|L_i u - p_{i,\ell}\|^2 + \sum_{j=1}^m \kappa_j \|F u - r_{j,\ell}\|^2$
- For $i = 1,\ldots,n$
  - $v_{i,\ell+1} = v_{i,\ell} + \lambda_\ell\big(L_i(2c_\ell - y_\ell) - p_{i,\ell}\big)$
- For $j = 1,\ldots,m$
  - $w_{j,\ell+1} = w_{j,\ell} + \lambda_\ell\big(F(2c_\ell - y_\ell) - r_{j,\ell}\big)$
- $y_{\ell+1} = y_\ell + \lambda_\ell(c_\ell - y_\ell)$

Assumption 3.4

1. $\Big(\bigcap_{i=1}^n \operatorname{ridom} f_i \circ L_i F^\top\Big) \cap \Big(\bigcap_{j=1}^m \operatorname{ridom} g_j\Big) \neq \varnothing$
   (resp. $\Big(\bigcap_{i=1}^n \operatorname{ridom} f_i \circ L_i\Big) \cap \Big(\bigcap_{j=1}^m \operatorname{ridom} g_j \circ F\Big) \neq \varnothing$*).*
2. *There exists* $\underline{\lambda} \in]0,2[$ *such that* $(\forall \ell \in \mathbb{N})$, $\underline{\lambda} \le \lambda_{\ell+1} \le \lambda_\ell$.
3. *(*$\forall i \in \{1,\ldots,n\}$*),* $\sum_{\ell\in\mathbb{N}} \|a_{i,\ell}\| < +\infty$ *and (*$\forall j \in \{1,\ldots,m\}$*),* $\sum_{\ell\in\mathbb{N}} \|b_{j,\ell}\| < +\infty$.

In these algorithms, a large-size matrix inversion must be performed for solving the quadratic minimization required in the initialization step and in the computation of the intermediate variables $(c_\ell)_{\ell\in\mathbb{N}}$. As shown next, the form of the frame operator F made in (8) renders this inversion tractable:

- for SF (Algorithm 1)

$$\begin{aligned}
&\kappa\Big(\sum_{i=1}^n \eta_i F L_i^\top L_i F^\top + \kappa \mathrm{I}\Big)^{-1}\\
&= \mathrm{I} - F\Big(\kappa\big(\sum_{i=1}^n \eta_i L_i^\top L_i\big)^{-1} + F^\top F\Big)^{-1} F^\top,\\
&= \mathrm{I} - F\Big(\kappa\big(\sum_{i=1}^n \eta_i L_i^\top L_i\big)^{-1} + \mu_U \sum_{q=1}^Q V_q^\top V_q\Big)^{-1} F^\top,
\end{aligned} \tag{19}$$

- for AF (Algorithm 2)

$$\begin{aligned}
&\Big(\sum_{i=1}^n \eta_i L_i^\top L_i + \kappa F^\top F\Big)^{-1}\\
&\qquad = \Big(\sum_{i=1}^n \eta_i L_i^\top L_i + \kappa\mu_U \sum_{q=1}^Q V_q^\top V_q\Big)^{-1}
\end{aligned} \tag{20}$$

by setting $\kappa = \sum_{j=1}^m \kappa_j$.

The last matrix inversions in (19) and (20) are easily performed by noticing that $(L_i)_{1\le i\le n}$ and $(V_q)_{1\le q\le Q}$ can be jointly decomposed by Fourier diagonalization techniques.

4. EXPERIMENTAL RESULTS

In this part, we apply the proposed optimization methods to image restoration. More specifically, we consider the following SF and AF problems:

$$\min_{x\in\mathbb{R}^K} f_1(TF^\top x) + \imath_C(F^\top x) + g_1(x) \tag{21}$$

and

$$\min_{y\in\mathbb{R}^N} f_1(Ty) + \imath_C(y) + g_1(Fy) \tag{22}$$

where F represents the 2-band DTT [20] which, as mentionned in Section 2.2, is a particular case of the frame operator subclass defined by (8), and where $T \in \mathbb{R}^{N\times N}$ denotes the matrix associated with a 2D (periodic) convolution operator. Problem (21) (resp. (22)) is a particular case of Problem (2) (resp. (3)) where $n = 2$ and $m = 1$. f_1 denotes the data fidelity term and $f_2 = \imath_C$ is the indicator function (see (13)) of a nonempty closed convex set C of $\mathbb{R}^N$ (for example, related to support or value range contraints). g_1 corresponds to the regularization term operating in the frame domain. In the considered problems, $L_1 = T$ and $L_2 = \mathrm{I}$. The matrices T and $(V_q)_{1\leq q\leq Q}$ (related to F) as defined above can be diagonalized by using a 2D Discrete Fourier Transform (DFT), in order to efficiently perform the matrix inversions in (19) and (20).

Some experiments are presented in Figures 1 and 2, for images degraded by Poisson noise with scaling factor $\alpha = 0.8$ and by a uniform blur of kernel size 3×3. The DTT [20] is computed using symlets of length 6 over 3 resolution levels. The data fidelity term f_1 corresponds to the generalized Kullback-Leibler divergence, which is well adapted to Poisson noise. Its proximity operator is derived from Example 3.2. $C = [0,255]^N$ models a constraint on the range of the pixel values and g_1 corresponds to a classical regularization of the form:

$$g_1 \colon (\xi_k)_{1\leq k\leq K} \mapsto \sum_{k=1}^{K} \tau_k |\xi_k|^{\beta_k}. \tag{23}$$

In our simulations, the parameters $(\tau_k)_{1\leq k\leq K} \in]0,+\infty[^K$ and $(\beta_k)_{1\leq k\leq K} \in \{1,4/3,3/2,2\}^K$ in (23) are empirically chosen to maximize the signal-to-noise-ratio (SNR). When $\beta_k \equiv 1$, the proximity operator of g_1 reduces to a soft thresholding as shown by Example 3.1.

Figure 1 shows a comparison between the use of a complex DTT and of a tight frame version of the complex DTT (where for every $q \in \{1,\ldots,4\}$, $V_q = \mathrm{I}$). In this simulation example, a cropped version of "Barbara" image ($N = 128\times 128$) is considered by adopting a SF criterion. The use of the non-tight DTT including prefilters allows us to improve the quality of the results both visually and in terms of SNR and SSIM [23].

Figure 2 displays a second restoration example on a cropped version of "Marseille" image ($N = 128\times 128$), still by considering DTT, both for the AF and SF criteria. The restoration results present slight differences in favour of the AF approach.

Original

Degraded: SNR = 11.4 dB , SSIM = 0.53

Tight-frame Complex DTT: SNR = 13.3 dB , SSIM = 0.69

Complex DTT: SNR = 14.2 dB , SSIM = 0.73

Figure 1: Cropped versions of Barbara image. Images are restored using SF and complex DTT.

REFERENCES

[1] D. L. Donoho. De-noising by soft-thresholding. *IEEE Trans. Inform. Theory*, 41(3):613–627, May 1995.

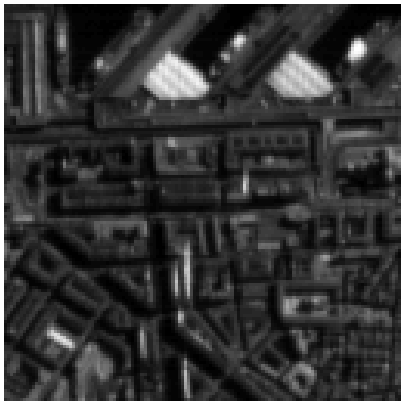

Original

Degraded: SNR = 14.0 dB , SSIM = 0.79

Restored SF: SNR = 16.3 dB , SSIM = 0.87

Restored AF: SNR = 16.6 dB , SSIM = 0.88

Figure 2: Synthesis approach versus Analysis approach.

[2] R. Coifman and D. Donoho. Translation-invariant de-noising. In A. Antoniadis and G. Oppenheim, editors, *Wavelets and Statistics*, volume 103 of *Lecture Notes in Statistics*, pages 125–150. Springer, New York, NY, USA, 1995.

[3] P. L. Combettes and V. R. Wajs. Signal recovery by proximal forward-backward splitting. *Multiscale Modeling and Simulation*, 4(4):1168–1200, Nov. 2005.

[4] I. Daubechies, M. Defrise, and C. De Mol. An iterative thresholding algorithm for linear inverse problems with a sparsity constraint. *Comm. Pure Applied Math.*, 57(11):1413–1457, 2004.

[5] M. A. T. Figueiredo and R. D. Nowak. An EM algorithm for wavelet-based image restoration. *IEEE Trans. Image Process.*, 12(8):906–916, Aug. 2003.

[6] J. Bect, L. Blanc-Féraud, G. Aubert, and A. Chambolle. A l^1-unified variational framework for image restoration. In T. Pajdla and J. Matas, editors, *Proc. European Conference on Computer Vision (ECCV)*, volume LNCS 3024, pages 1–13, Prague, Czech Republic, May 2004. Springer.

[7] C. Chaux, P. L. Combettes, J.-C. Pesquet, and V. R. Wajs. A variational formulation for frame-based inverse problems. *Inverse Problems*, 23:1495–1518, June 2007.

[8] P. L. Combettes and J.-C. Pesquet. A Douglas-Rachford splitting approach to nonsmooth convex variational signal recovery. *IEEE J. Selected Topics Signal Process.*, 1(4):564–574, Dec. 2007.

[9] P. L. Combettes and J.-C. Pesquet. A proximal decomposition method for solving convex variational inverse problems. *Inverse Problems*, 24(6):x+27, Dec. 2008.

[10] M. Afonso, J. Bioucas-Dias, and M. A. T. Figueiredo. An augmented lagrangian approach to the constrained optimization formulation of imaging inverse problems. *IEEE Trans. Image Process.*, 2009. http://arxiv.org/abs/0912.3481, submitted.

[11] S. Setzer, G. Steidl, and T. Teuber. Deblurring poissonian images by split Bregman techniques. *J. Vis. Comm. Image Repr.*, 21:193–199, 2010.

[12] M. Elad, P. Milanfar, and R. Ron. Analysis versus synthesis in signal priors. *Inverse Problems*, 23(3):947–968, June 2007.

[13] L. Chaâri, N. Pustelnik, C. Chaux, and J.-C. Pesquet. Solving inverse problems with overcomplete transforms and convex optimization techniques. In *SPIE*, San Diego, CA, Aug. 2-4 2009.

[14] M. Carlavan, P. Weiss, L. Blanc-Féraud, and J. Zerubia. Algorithme rapide pour la restauration d'image régularisée sur les coefficients d'ondelettes. In *Proc. GRETSI*, Dijon, Sept., 8-11 2009.

[15] E. J. Candès and D. L. Donoho. Recovering edges in ill-posed inverse problems: Optimality of curvelet frames. *Ann. Stat.*, 30:784–842, 2002.

[16] I. Daubechies. *Ten lectures on wavelets*. CBMS-NSF Lecture Notes nr. 61. SIAM, 1992.

[17] M. N. Do and M. Vetterli. The contourlet transform: an efficient directional multiresolution image representation. *IEEE Trans. Image Process.*, 14(12):2091–2106, Dec. 2005.

[18] D. Han and D. R. Larson. Frames, bases, and group representations. *Mem. Amer. Math. Soc.*, 147(697):x+94, 2000.

[19] N. G. Kingsbury. Complex wavelets for shift invariant analysis and filtering of signals. *Appl. Comp. Harm. Analysis*, 10(3):234–253, May 2001.

[20] C. Chaux, L. Duval, and J.-C. Pesquet. Image analysis using a dual-tree *M*-band wavelet transform. *IEEE Trans. Image Process.*, 15(8):2397–2412, Aug. 2006.

[21] J. J. Moreau. Proximité et dualité dans un espace hilbertien. *Bull. Soc. Math. France*, 93:273–299, 1965.

[22] J.-C. Pesquet. A parallel inertial proximal optimization method. Preprint, 2010.

[23] Z. Wang and A. C. Bovik. Mean squared error: love it or leave it? *IEEE Signal Processing Magazine*, 26(1):98–117, Jan. 2009.